

Two-band superconductivity in Pb from *ab initio* calculations

A. Floris,¹ A. Sanna,² S. Massidda,² and E. K. U. Gross¹

¹*Institut für Theoretische Physik, Freie Universität Berlin, Arnimallee 14, D-14195 Berlin, Germany*
²*INFM SLACS, Sardinian Laboratory for Computational Materials Science and Dipartimento di Scienze Fisiche, Università degli Studi di Cagliari, S.P. Monserrato-Sestu km 0.700, I-09124 Monserrato (Cagliari), Italy*

(Received 31 October 2006; published 9 February 2007)

We perform first-principles calculations of the band and k -point resolved superconducting gap of Pb in the framework of the density functional theory for superconductors. Without any adjustable parameter or assumption different from s -wave symmetry, we find two different values of the gap on the two sheets of the Fermi surface, which can be related to the different electron-phonon couplings characterizing the electronic states in the corresponding bands. These, in turn, derive from the different orbital character of the electronic states. We also find some intraband gap anisotropy in each Fermi surface sheet. Our calculated gap, critical temperature and total anisotropy of the gap are in good agreement with tunneling experiments. We estimate an $\approx 8\%$ enhancement of T_c coming from the gap anisotropy. However, the experimentally found T^3 temperature dependence of the specific heat cannot be found within our assumed anisotropic s -wave gap symmetry.

DOI: [10.1103/PhysRevB.75.054508](https://doi.org/10.1103/PhysRevB.75.054508)

PACS number(s): 74.25.Jb, 74.25.Kc, 74.70.Ad

I. INTRODUCTION

The possibility of multiband superconductivity was discussed¹ already a few years after the formulation of the Bardeen-Cooper-Schrieffer (BCS) theory² and later reported in several experimental papers.^{3–5} Moreover, the dependence of the superconducting (SC) gap on the direction in k -space was analyzed for different materials, like Pb (Refs. 6–8) and Sn.⁹ The recent discovery of two-gap superconductivity (TGSC) in MgB₂ brought this problem back to the attention of the scientific community. Theoretical and experimental investigations on MgB₂ have emphasized how important the presence of multiple gaps can be to enhance the critical temperature T_c of a specific material. Theoretical estimates have in fact shown that retaining the information about the σ , π band dependence of the electron-phonon interaction in MgB₂ greatly enhances the calculated T_c , relative to an averaged, single-band, calculation.^{10–13} Of crucial importance is the question: How and when does multigap superconductivity increase T_c ? In this context, it is very interesting to investigate the gap anisotropy in different materials showing this peculiarity. Pb is such a material: the unconventional aspects of its superconductivity, relative to BCS, have been discussed in several papers.^{6–8,14,15,30–32} In particular, two separated SC gaps have been found experimentally^{14,15} and investigated theoretically.^{6,7}

Very recently, an approach to superconductivity, based on density functional theory (SCDFT)^{16,17} has been able, in a completely parameter-free fashion, to describe successfully the superconducting properties of several materials, ranging from weak and intermediate to the strong coupling regime^{13,16,17} and from ambient to high pressure conditions.^{18,19} Unlike within Eliashberg theory, the Coulomb interaction is included in the calculation on the same footing as the electron-phonon interaction. This proved to be very important in MgB₂, where a band resolved treatment of the Coulomb repulsion resulted to be crucial to reproduce the T_c of this material from first principles.¹³ These considerations show that a theory with a predictive character as

SCDFT, retaining the full band dependence and anisotropy of the SC gap, can prove to be very useful to study TGSC.

In this work, we use a fully (n, \mathbf{k}) -resolved formalism within SCDFT and calculate from first principles the SC properties. Although a generalization to general symmetry is possible, our present formulation still assumes an anisotropic s symmetry for the order parameter. Within this approach all the features of the SC gap emerge naturally, without any *a priori*, material specific, physical model and without adjusting any parameter. Our results confirm the experimental finding that Pb is a two band superconductor. The calculated gaps, their overall anisotropy, and the T_c result in good agreement with experiments reported in Refs. 14 and 15 and with previous calculations.^{6,7} A T_c enhancement of $\approx 8\%$ can be directly related to a gap anisotropy $|\Delta_2 - \Delta_1|/\Delta_{\text{iso}} \approx 20\%$, much smaller than that of MgB₂. Here Δ_1 , Δ_2 are the averaged gap inside each band and Δ_{iso} is the average gap resulting from an isotropic interaction. The ratios $2\Delta_{1,2}/K_B T_c$ are in very good agreement with the corresponding experimental values. Moreover, anisotropy slightly changes the temperature dependence of the electronic specific heat, but cannot reconcile the calculations with the T^3 dependence reported experimentally (Ref. 31). The existence of the two gaps and their intraband anisotropy are related to the corresponding anisotropy of the electron-phonon (e -ph) coupling in the two bands crossing the Fermi level, which strongly correlates with the s and d character of the bands.

The paper is organized as follows: In Sec. II we summarize the main features of the SCDFT. In Sec. III we describe the computational details of our calculation. Our main results are presented and analyzed in Sec. IV, and finally in Sec. V, we draw our conclusions.

II. DENSITY FUNCTIONAL THEORY FOR SUPERCONDUCTORS

The central result of the SCDFT is the generalized gap equation

$$\Delta_{nk} = -Z_{nk}\Delta_{nk} - \frac{1}{2} \sum_{n'k'} \mathcal{K}_{nk,n'k'} \frac{\tanh\left(\frac{\beta}{2}E_{n'k'}\right)}{E_{n'k'}} \Delta_{n'k'}. \quad (1)$$

In this self-consistent equation, n and \mathbf{k} are, respectively, the electronic band index and the Bloch wave vector; Δ_{nk} represents the SC gap function; β is the inverse temperature; $E_{nk} = \sqrt{(\varepsilon_{nk} - \mu)^2 + |\Delta_{nk}|^2}$ are the SC quasiparticle energies, defined in terms of the gap function, the Kohn-Sham eigenenergies ε_{nk} of the normal state and the chemical potential μ . The *universal* kernel $\mathcal{K}_{nk,n'k'}$ appearing in Eq. (1) consists of two contributions $\mathcal{K} = \mathcal{K}^{e\text{-ph}} + \mathcal{K}^{e\text{-e}}$, representing the effects of the e -ph and the e - e interactions, respectively. $\mathcal{K}^{e\text{-ph}}$ is temperature dependent and involves the e -ph coupling matrix elements $|g_{k,k',v}^{nm'}|^2$ and the phonon spectrum ω_{qv} , while $\mathcal{K}^{e\text{-e}}$ contains the matrix elements of the screened Coulomb repulsion. Equation (1) has the same structure as the BCS gap equation, with the kernel \mathcal{K} replacing the model interaction of BCS theory. This similarity allows us to interpret \mathcal{K} as an effective interaction, responsible for the binding of the Cooper pairs. Finally, the *universal* diagonal (and temperature dependent) term Z_{nk} plays a similar role as the renormalization term in the Eliashberg equations. We emphasize that Eq. (1) is not a mean-field equation (as in BCS theory), since it contains correlation effects via the SC exchange-correlation (xc) functional entering \mathcal{K} and Z . Furthermore, it has the form of a static equation—i.e., it does not depend *explicitly* on the frequency—and therefore has a simpler structure (and computationally more manageable) than the Eliashberg equations. However, this certainly does not imply that retardation effects are absent from the theory. Once again, retardation effects enter through the xc functional, as explained in Refs. 16 and 17.

An important point of our approach is the capability of including the Coulomb repulsion *ab initio*, without any adjustable parameter. So far,^{13,16–19} we used a Thomas-Fermi approximation for screening the e - e repulsion. In this paper we use the static dielectric matrix, within the RPA (Ref. 20). Our results show a good agreement between the RPA and Thomas-Fermi results, consistent with the s - p nature of valence states of Pb.

III. COMPUTATIONAL DETAILS

The solution of Eq. (1) requests the preliminary calculation of the normal state band structure ε_{nk} of the material, the phonon spectrum ω_{qv} , and the e -ph and Coulomb matrix elements (ME) with respect to the Bloch functions. As the accuracy of the calculated density of states at the Fermi level is crucial in the formalism, band structure calculations were performed within the all-electron FLAPW method²¹ at the experimental lattice constant ($a=9.35$ a.u.). The phonon spectrum and the e -ph ME were calculated at the LDA theoretical lattice constant ($a=9.03$ a.u.) by density functional perturbation theory,²² within the plane-wave-pseudopotential method.²³ We made use of a norm conserving pseudopotential, including the scalar-relativistic correction.²⁴ An energy cutoff of 32 Ry and a 26^3 Monkhorst-Pack \mathbf{k} -point mesh

were sufficient to achieve a very good convergence of the phonon spectrum, e -ph coupling and SC gap. Our calculated phonon spectrum is almost identical to the results of previous calculations.²⁵ Moreover, we find a good agreement with available experiments,²⁶ although a small but not negligible overestimate of the calculated frequencies is present, in particular around the X point and along the XK symmetry line of the Brillouin zone.^{25,28} This effect significantly affects the value of our calculated total e -ph λ . We will comment on this point later. The phonon calculations at the experimental lattice constant strongly underestimate the phonon frequencies. This fact motivates our choice to calculate the spectrum at the theoretical lattice constant, since the values of the SC gap and T_c are extremely sensitive (via the e -ph coupling) to the phonon spectrum. We calculated the phonon frequencies on a regular mesh of 8^3 \mathbf{q} points, after verifying, against denser mesh, that this grid was sufficient to capture all features of the SC gap. We included the RPA screened Coulomb ME, calculated on a mesh of $9^3 \times 9^3$ \mathbf{k} and \mathbf{k}' points.

We solved the SCDFT gap equation in two cases: (i) including the full (n, \mathbf{k}) -resolved e -ph ME $|g_{k,k',v}^{nm'}|^2$ and (ii) including only their average on the Fermi surface, through the Eliashberg function $\alpha^2F(\omega)$. The SC gap function is extremely peaked around the Fermi surface, whereas at higher energies it is rather smooth (and negative, due to the e - e interaction). This implies that a converged solution of Eq. (1) needs a denser \mathbf{k} -points sampling around E_F , and coarser elsewhere. This highly nonuniform mesh of the BZ is realized with 6×10^3 and 500 independent \mathbf{k} points for bands crossing and not crossing the Fermi level, respectively. Finally, 15–20 self-consistent iterations were sufficient to achieve a complete convergence of the gap.

IV. RESULTS

The set of black points in Fig. 1 shows the gap at $T=0$ K, as a function of the energy distance from the Fermi level E_F . An important feature of the plot is that for each energy the gap is not a single-valued function. This means that, in general, the SC gap is not isotropic in the reciprocal space, i.e., for $\varepsilon=E_F$ its value depends on the Fermi vector \mathbf{k}_F . In particular, for each $\varepsilon \approx E_F$ we observe two distinct “sets” of gaps, in strict analogy with the case of MgB₂ (see, for comparison, Fig. 1 in Ref. 13). Moreover, each “set” has an associated, finite, vertical energy spread. In Fig. 2(a) we plot the Fermi surface (FS) of lead. It consists of two sheets, coming from the two (essentially p) bands crossing E_F . The sheets are topologically quite different, the first one being rather spherical, the second having a more complex tubular-like structure. The colors in Fig. 2(a) represent the values of Δ_{nk_F} . It is clear that the two distinct sets of Δ in Fig. 1 come from the two sheets of the Fermi surface. Figure 1 shows that their energy separation is in excellent agreement with the experiments,^{14,15} although our calculated gap values are slightly underestimated.

We should comment here on this difference, related to the calculation of the e -ph coupling. We obtained $\lambda=1.3$, to be compared with $\lambda_{\text{EXP}}=1.55$ as measured by tunneling

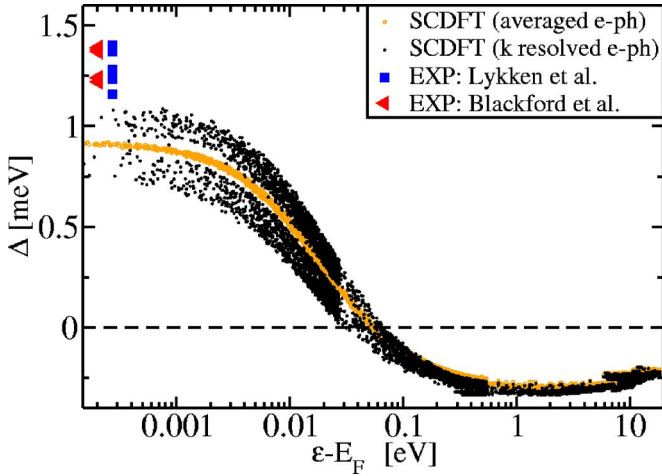


FIG. 1. (Color online) Superconducting gap of Pb as a function of the energy distance from the Fermi energy ($T=0$ K). Small black points: Δ resulting from the inclusion of the \mathbf{k} -resolved e -ph and Coulomb matrix elements. Small gray (orange) points: Δ calculated with a corresponding averaged e -ph interaction [Eliashberg function $\alpha^2F(\omega)$]. Big triangles and squares: experimental values (from Refs. 14 and 15).

experiments.²⁷ As already mentioned, our underestimate value of λ is mostly related to the overestimate of the phonon frequencies along the XK symmetry line in the BZ. This leads to an upward shift of the two peaks in the Pb Eliashberg function (not shown). This shift (present, in the transverse branch, in all previous works^{25,28,29}) has been related^{28,29} to the absence of the spin-orbit coupling effect in the calculation. In our results the shift of the phonon frequencies relative to the experiment²⁶ is $\approx 5 \text{ cm}^{-1}$ in all the three branches. Unfortunately, the calculation of the electron-phonon coupling within a fully relativistic approach is not easy and, to our knowledge, has not been achieved so far. In any case, our $\lambda=1.3$ compares very well with other theoretical estimates (Carbotte *et al.*, $\lambda=1.32$;⁷ Liu *et al.*, $\lambda=1.2$),²⁸ although it is quite distant from Savrasov *et al.* $\lambda=1.68$.²⁹ Our previous results of Ref. 17 used the $\alpha^2F(\omega)$ of Ref. 29. We stress that because of the absence in our calculation of adjustable parameters, any error in the calculation of λ (due to inaccuracies of the phonon spectrum or of the e -ph ME themselves) shows up dramatically in the superconducting properties, due the intrinsically exponential dependence of T_c on the couplings. Within Eliashberg theory, on the other hand, different λ values are normally adjusted by changing μ^* .

Figure 2(a) also shows that Δ_{nk} is anisotropic inside each single sheet, resulting in the vertical energy spread mentioned before (intragap anisotropy). Continuing our analysis, in Fig. 2(b) we plot the e -ph coupling λ_{nk_F} on the FS, where

$$\lambda_{nk} = 2 \sum_{n'k',\nu} \frac{|g_{k,k',\nu}^{nn'}|^2}{\omega_{k'-k,\nu}} \times \delta(\varepsilon_{n'k'} - E_F) \quad (2)$$

is the average of all the possible e -ph scattering processes connecting two points at FS, but always involving the elec-

tronic initial state (n, \mathbf{k}) . The total e -ph coupling constant λ can be expressed as $\lambda = \frac{1}{N(E_F)} \sum_{nk} \lambda_{nk} \times \delta(\varepsilon_{nk} - E_F)$. Comparing the plots in Fig. 2(a) and Fig. 2(b) we notice a striking similarity, that indicates a strong correlation between the n dependence and \mathbf{k} anisotropy of the e -ph coupling and of the gap. Moreover, our calculations show that the gap anisotropy is due to the e -ph coupling only: the open gray (orange, color online) symbols in Fig. 1 show the gap function calculated with an average e -ph interaction, i.e., including the phononic kernels \mathcal{K}^{e-ph} and \mathcal{Z} that contain the Eliashberg function $\alpha^2F(\omega)$ [see Eqs. (23) and (24) of Ref. 17], but still with the Coulomb ME $\mathcal{K}_{nk,n'k'}^{e-e}$. It is clear that the e -ph average washes out all the band and direction dependence of the gap [i.e., $\Delta_{nk} = \Delta(\varepsilon_{nk})$]. We note in passing that the two calculations are fully consistent in that the gap from the averaged e -ph coupling is very close to the DOS-weighted average of the anisotropic Δ_{nk} on the two FS sheets.

The different e -ph coupling in the two sheets, $\lambda_{1k_F} = 0.8-1.1$, $\lambda_{2k_F} = 1.24-1.7$, is related to the slightly different character of the corresponding two bands (see Fig. 3). While the “spherical” sheet has a mixed s - p character, the tubular one is more p - d -like. Moreover, comparing Fig. 2(a) with Fig. 3 we notice a striking correlation between d -character (s character) and higher (lower) gap values. These results are reminiscent of our previous calculations on Li and K under pressure,^{18,19} where we found that more localized electronic states are more coupled with the ionic system, producing a correspondingly higher SC gap.

Equation (1) allows to calculate Δ_{nk} as a function of temperature T , defining T_c from the condition that $\Delta_{nk}(T_c) = 0$. Figure 4(a) shows the two (intragap averaged) gaps at E_F as a function of T . We obtain $T_c = 5.25$ K and $T_c = 4.84$ K for the anisotropic and average calculation, respectively. The full consistence between the two calculations allows us to draw conclusions from the comparison of results. In fact, we see that the weighted average of the Δ values on the two bands nearly coincides at $T=0$ K with the result obtained averaging the \mathbf{k} dependence of e -ph couplings. We see that, although certainly not in a proportion comparable with MgB_2 , the presence of an anisotropic, multiband gap produces an 8% enhancement of the value of T_c . Clearly, in MgB_2 this effect is crucial,¹⁰⁻¹³ whereas here it is much smaller. This is partially due to the much lower difference in e -ph coupling between the two bands and the resulting values of the gaps (in MgB_2 the coupling in the σ bands is roughly 3 times higher than in the π bands). An interesting question is under which conditions does a system show multiband superconductivity, i.e., with a clear separation between the gaps. Looking again at the λ_{nk_F} we see that in Pb the two sets corresponding to the two bands crossing E_F are not contiguous, i.e., the values of λ_{1k_F} and λ_{2k_F} do not superimpose. In order to check whether the presence of two separate gaps is related directly to this property of the λ_{nk_F} , we performed several model calculations, rescaling the e -ph ME, in order to have a continuous set of λ_{nk_F} and keeping constant the value of the total, average λ . It turned out that the two SC gaps Δ_{nk_F} get contiguous exactly when the two set of λ_{nk_F} do, independently of the details of how the coupling were

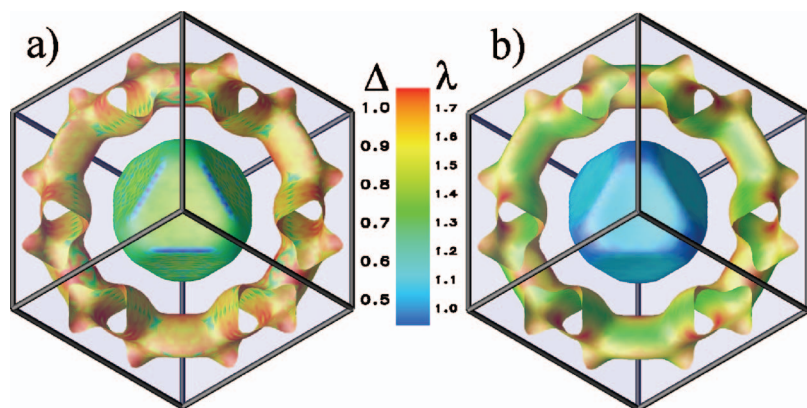


FIG. 2. (Color) (a) Superconducting gap Δ_{nk} calculated at the Fermi surface of Pb, at $T=0$ K. (b) Electron-phonon interaction λ_{nk} at FS.

modified to bring the λ_{nk_F} to merge. Leaving open the question on whether or not this coincidence is a general feature, we conclude that Pb is a two gap system due to the fact that λ_{nk_F} are disjoint sets (relative to the band n). In particular, as already pointed out, the Coulomb repulsion does not seem to play an important role in both the interband and intraband anisotropy of the gap.

In order to analyze further our results, it is interesting to plot our data and the experimental values normalized to its own T_c , in such a way as to immediately compare in the ordinate with the value of $2\Delta/K_B T_c = 3.52$ predicted by BCS theory. We first notice that both gaps yield $2\Delta/K_B T_c > 3.52$, in agreement with the strong coupling nature of Pb. We also notice that the full account of anisotropy gives the $2\Delta_{1,2}/K_B T_c$ ratios in very good agreement with the experimental values.

Finally, we calculated the electronic specific heat in the

SC state C_{es} as a function of temperature. According to experiments, C_{es} follows a T^3 law for $T < 1.5$ K (Ref. 31), and for $1 \text{ K} < T < 4 \text{ K}$,³⁰ instead of a BCS-exponential law. Several attempts to explain this anomaly can be found in the literature, focusing on the role of the gap anisotropy,³¹ and its relation to the existence of a spin-density wave.³² In Fig. 5 we present our calculated C_{es} in both the isotropic and anisotropic case: Although we do not find a T^3 law for $T < 1.5$ K in the anisotropic case (our SC gap does not have nodes on the FS), the anisotropy produces a deviation (in the direction of experiments) from the BCS-like plot, starting from $T \approx 4$ K. Our calculations agree fairly well with the measurements in dirty samples. However, considering that the calculated gap anisotropy is comparable to the experimental one, we conclude that the gap anisotropy is not sufficient to explain the experimental C_{es} anomaly, at least with our assumed anisotropic s symmetry.

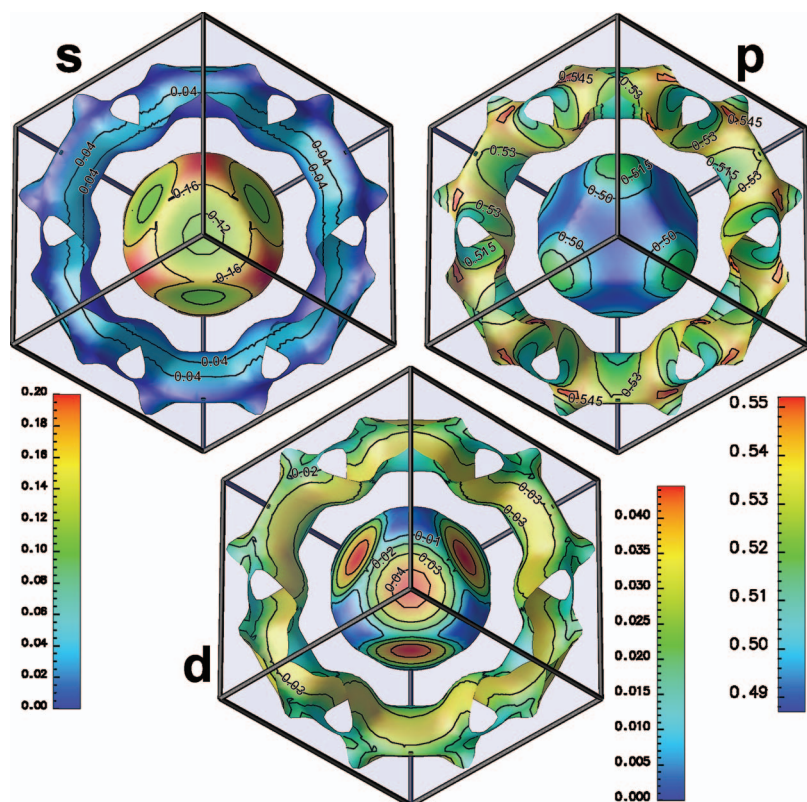


FIG. 3. (Color) Characters of the wave functions on the FS.

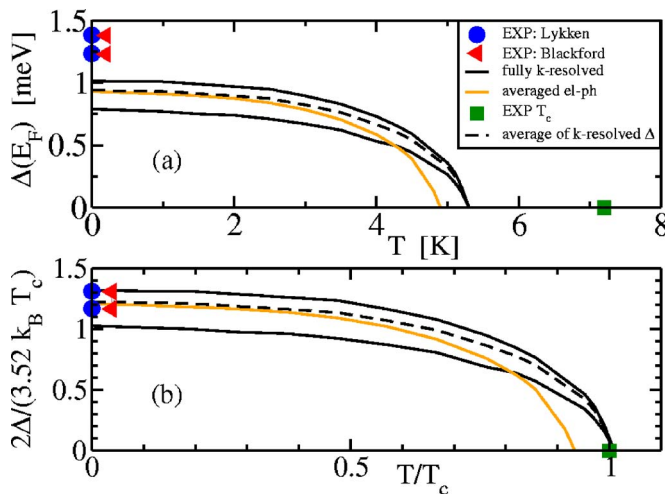


FIG. 4. (Color online) (a) Calculated and experimental superconducting gaps of Pb as a function of T . (b) Same data renormalized using the calculated (fully anisotropic calculation) and experimental T_c , respectively. Unity values on the ordinate would correspond to the BCS result.

V. CONCLUSIONS

In this paper we report first-principles calculations of the superconducting gap of Pb, using the density functional theory for superconductors within a (n, k) -resolved approach. Without assuming any *ad-hoc* model or adjustable parameter, we find that Pb is a two-gap material, in agreement with available experiments and previous theoretical results based on other methods. We show that the n and k gap anisotropy and the separation of the two gaps correlate strongly with the anisotropy of the electron-phonon interaction, and that the latter is connected with the wave function characters on the different sheets of the Fermi surface. The multigap character produces an enhancement of T_c relative to

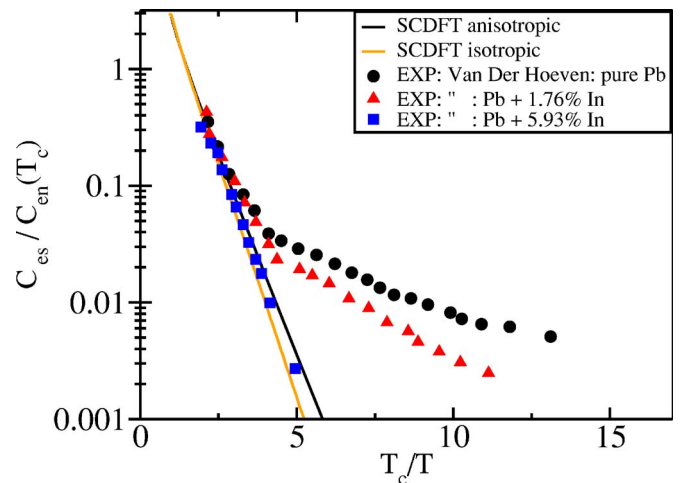


FIG. 5. (Color online) Normalized temperature dependence of the electronic specific heat in the SC state. Different symbols refer to experiments in pure and In-doped samples (Ref. 31).

the isotropic case, although this effect is not so dramatic as in MgB_2 . Finally, we calculated the specific heat, discussing its temperature dependence compared to the experiments. The experimental T^3 behavior cannot be found within our approach.

ACKNOWLEDGMENTS

The authors thank Andrea Marini for useful discussions and for his help. This work was supported by the Italian Ministry of Education, under the projects PRIN 2006021741 and PONCyberSar, by the Istituto Nazionale di Fisica della Materia (INFM-CNR) through a supercomputing grant at Cineca (Bologna, Italy), by the Deutsche Forschungsgemeinschaft, by the EXCITING Network and by the NANOQUANTA Network of Excellence.

- ¹H. Suhl, B. T. Matthias, and L. R. Walker, Phys. Rev. Lett. **3**, 552 (1959).
- ²J. Bardeen, L. N. Cooper, and J. R. Schrieffer, Phys. Rev. **108**, 1175 (1957).
- ³L. Y. L. Shen, N. M. Senozan, and N. E. Phillips, Phys. Rev. Lett. **14**, 1025 (1965).
- ⁴R. Radebaugh and P. H. Keesom, Phys. Rev. **149**, 209 (1966).
- ⁵G. Binnig, A. Baratoff, H. E. Hoenig, and J. G. Bednorz, Phys. Rev. Lett. **45**, 1352 (1980).
- ⁶A. J. Bennett, Phys. Rev. **140**, A1902 (1965).
- ⁷P. G. Tomlinson and J. P. Carbotte, Phys. Rev. B **13**, 4738 (1976).
- ⁸J. D. Short and J. P. Wolfe, Phys. Rev. Lett. **85**, 5198 (2000).
- ⁹N. V. Zavaritskii, Zh. Eksp. Teor. Fiz. **45**, 1839 (1963) [Sov. Phys. JETP **18**, 1260 (1964)].
- ¹⁰A. Y. Liu, I. I. Mazin, and J. Kortus, Phys. Rev. Lett. **87**, 087005 (2001).
- ¹¹H. J. Choi, D. Roundy, H. Sun, M. L. Cohen, and S. G. Louie, Phys. Rev. B **66**, 020513(R) (2002).

- ¹²H. J. Choi, D. Roundy, H. Sun, M. L. Cohen, and S. G. Louie, Nature (London) **418**, 758 (2002).
- ¹³A. Floris, G. Profeta, N. N. Lathiotakis, M. Lüders, M. A. L. Marques, C. Franchini, E. K. U. Gross, A. Continenza, and S. Massidda, Phys. Rev. Lett. **94**, 037004 (2005).
- ¹⁴B. L. Blackford and R. H. March, Phys. Rev. **186**, 397 (1969).
- ¹⁵G. I. Lykken, A. L. Geiger, K. S. Dy, and E. N. Mitchell, Phys. Rev. B **4**, 1523 (1971).
- ¹⁶M. Lüders, M. A. L. Marques, N. N. Lathiotakis, A. Floris, G. Profeta, L. Fast, A. Continenza, S. Massidda, and E. K. U. Gross, Phys. Rev. B **72**, 024545 (2005).
- ¹⁷M. A. L. Marques, M. Lüders, N. N. Lathiotakis, G. Profeta, A. Floris, L. Fast, A. Continenza, E. K. U. Gross, and S. Massidda, Phys. Rev. B **72**, 024546 (2005).
- ¹⁸G. Profeta, C. Franchini, N. N. Lathiotakis, A. Floris, A. Sanna, M. A. L. Marques, M. Lüders, S. Massidda, E. K. U. Gross, and A. Continenza, Phys. Rev. Lett. **96**, 047003 (2006).
- ¹⁹A. Sanna, C. Franchini, A. Floris, G. Profeta, N. N. Lathiotakis,

- M. Lüders, M. A. L. Marques, E. K. U. Gross, A. Continenza, and S. Massidda, *Phys. Rev. B* **73**, 144512 (2006).
- ²⁰SELF code, <http://www.fisica.uniroma2.it/~self/>.
- ²¹EXCITING code, <http://exciting.sourceforge.net/>.
- ²²S. Baroni, S. de Gironcoli, A. Dal Corso, and P. Giannozzi, *Rev. Mod. Phys.* **73**, 515 (2001).
- ²³Plane-wave self-consistent-field (PWSCF) code, <http://www.pwscf.org/>.
- ²⁴G. B. Bachelet, D. R. Hamann, and M. Schlüter, *Phys. Rev. B* **26**, 4199 (1982).
- ²⁵S. de Gironcoli, *Phys. Rev. B* **51**, 6773 (1995).
- ²⁶B. N. Brockhouse, T. Arase, G. Cagliotti, K. R. Rao, and A. D. B. Woods, *Phys. Rev.* **128**, 1099 (1962).
- ²⁷W. L. McMillan and J. M. Rowell, in *Superconductivity*, edited by R. D. Parks (Marcel Dekker, New York, 1969).
- ²⁸A. Y. Liu and A. A. Quong, *Phys. Rev. B* **53**, R7575 (1996).
- ²⁹S. Y. Savrasov and D. Y. Savrasov, *Phys. Rev. B* **54**, 16487 (1996).
- ³⁰M. Horowitz, A. A. Silvidi, S. F. Malaker, and J. G. Daunt, *Phys. Rev.* **88**, 1182 (1952).
- ³¹B. J. C. Van Der Hoeven, Jr. and P. H. Keesom, *Phys. Rev.* **137**, A103 (1965).
- ³²A. W. Overhauser and L. L. Daemen, *Phys. Rev. Lett.* **61**, 1885 (1988).